

Concurrence of bulk and surface order reconstruction to the relaxation of frustrated nematics

Antonino Amoddeo

Department of Civil, Energy, Environmental and Materials Engineering, Università “Mediterranea” di Reggio Calabria, Via Graziella 1, Feo di Vito, I-89122 Reggio Calabria, Italy

E-mail: antonino.amoddeo@unirc.it

Abstract. Applying appropriate electric pulses to a nematic liquid crystal confined between plates, the bulk order reconstruction can occur, a mechanism allowing the switching between topologically different nematic textures without any director rotation. Using a moving mesh finite element method we describe the order tensor dynamics for a nematic inside an asymmetric π -cell, putting in evidence as textural distortions induced by strong asymmetries can be relaxed via both bulk and surface order reconstruction, occurring close to a confining plate with different time duration.

1. Introduction

Nematic Liquid Crystals (NLCs) confined between flat glass plates, in presence of appropriate electric and mechanical stresses can experience textural modifications relaxing the induced distortion [1]. In a similar device, the π -cell, the plates are treated in order to impose an initial orientation to the adhered nematic molecules, commonly known as the pre-tilt angle. The electro-optical properties of nematics depend on their morphology, as they are rod-like molecules exhibiting orientational order and cylindrical symmetry. A unit vector, the director \mathbf{n} , accounts for the orientation of the NLC long axis, while the scalar order parameter S describes the degree of order along such direction, and their behaviour, if the applied distortions have length scales comparable to the biaxial coherence length ξ_b [2], becomes biaxial, as two distinct optical axes arise. Biaxial phenomena in NLCs have been extensively investigated, both experimentally and theoretically, see [3-6] and references therein, due to their role in the switching properties of electronic devices such as Liquid Crystal Displays (LCDs), which theoretical description requires the coupling of the \mathbf{n} and S parameters within the frame of the Landau-de Gennes order tensor \mathbf{Q} theory [7].

In fig. 1 we depict a π -cell, in which a thin film of nematic material is confined between the upper and lower glass plates, with pre-tilt angles θ_U and θ_L , respectively, generating a splayed texture [1], figure 1(a). The cell is said symmetric because $\theta_U = \theta_L$, otherwise it is asymmetric; both θ_U and θ_L are measured with respect to the internal face of each plate. An electric field applied perpendicularly to the boundary plates, cause the initial splay texture to be switched into the topological different π -bent one, figure 1(c), through the intermediate state of figure 1(b), where the biaxial order reconstruction take place in the cell centre: here, the two uniaxial textures depicted in figure 1(a) and 1(c) are connected through a wealth of transient biaxial states in the nanometric scale, allowing the local order of the nematic phase to change without any macroscopic director rotation [1].



The modelling of the \mathbf{Q} -tensor dynamics inside a π -cell containing a NLC results in a Partial Differential Equations (PDEs) system, solved using the Finite Element Method (FEM) implementing an adaptive grid numerical technique, the Moving Mesh Partial Differential Equation (MMPDE) [3-6]. Briefly, the domain discretization with an appropriate grid of points, typical of the FEM technique, is controlled according the monitor parameter $\nabla\mathbf{Q}$, while nodal connectivity and number of mesh points inside the domain are kept constant.

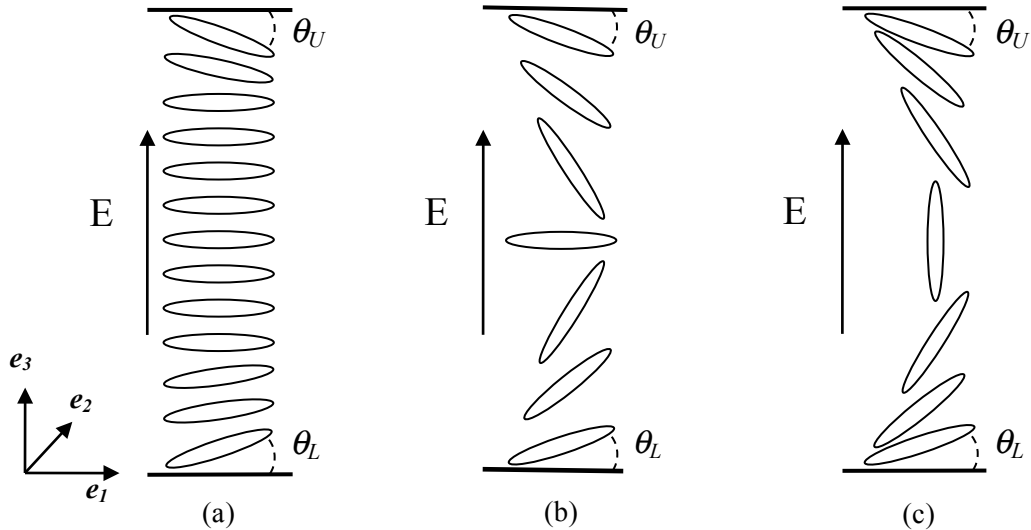


Figure 1. Outline of the π -cell with nematic molecules in different states: (a) horizontal alignment with a slight splay; (b) intermediate state, with a thin biaxial wall in the centre; (c) mostly vertical alignment (π -bent).

This allows the node points on which the PDE system is solved to be clustered into regions of high spatial variability where more detail is required, and it results an efficient and effective numerical tool appropriate to model the order dynamics of NLCs confined between plates, and the dynamics of complex systems more in general, as biological ones [8,9]. We present a MMPDE computation of the biaxial order dynamics for a 5CB NLC confined in an asymmetric π -cell, focusing on the switching mechanisms relaxing the nematic distortion. Throughout the simulations we neglect any material flow effect, as we are interested only determining the order evolution within the applied electric pulse duration, in which the order reconstruction transition is always confined [6,10].

2. Basic model

We assume that inside the π -cell, the free energy functional F , because of the infinite anchoring energy, has contributions coming from the bulk only, which are distinguished in electric, elastic and thermotropic ones, respectively F_e , F_d , and F_t . The second rank order tensor \mathbf{Q} , expressed in the orthonormal basis of its eigenvectors $\{e_1, e_2, e_3\}$ [7,11], describes both orientation and order of the NLC: the uniaxial nematic phase is characterized by the eigenvector $e_i = \mathbf{n}$ associated to s_{max} ; when all the three eigenvalues are different, the calamitic molecules are in the biaxial phase, on the contrary if they vanish the NLCs are in the isotropic phase. Neglecting ion effects and imposing the balance between F and the dissipation function D , the generalized Euler-Lagrange equations are obtained for each of the five independent parameters q_i corresponding to the degrees of freedom of a rod-like nematic molecule,

$$\frac{\partial \mathbf{D}}{\partial \dot{q}_i} + \frac{\partial F_t}{\partial q_i} + \frac{\partial F_e}{\partial q_i} + \frac{\partial F_d}{\partial q_i} - \frac{\partial}{\partial x_j} \left(\frac{\partial F_d}{\partial q_{i,j}} \right) - \frac{\partial}{\partial x_j} \left(\frac{\partial F_e}{\partial q_{i,j}} \right) = 0 \quad i=1\dots 5 \quad (1)$$

where j denotes differentiation with respect to the spatial coordinates, and summation over repeated indices is assumed. The electric potential U , entering in \mathbf{F} through F_e , is governed by

$$\nabla \cdot \mathbf{D} = \nabla \cdot (-\varepsilon_0 \boldsymbol{\varepsilon} \nabla U + \mathbf{P}_S) = 0 \quad (2)$$

in which \mathbf{D} is the displacement field, ε_0 is the vacuum dielectric permeability, $\boldsymbol{\varepsilon}$ is the dielectric tensor and \mathbf{P}_S is the spontaneous polarization vector. To solve the six coupled PDEs (1) and (2), due to the infinite anchoring energy of the nematic molecules we impose essential boundary conditions on the confining plates, obtaining the dynamical evolution of the system. The induced biaxial order is evaluated from [1]

$$\beta^2 = 1 - 6 \frac{\text{tr}(\mathbf{Q}^3)^2}{\text{tr}(\mathbf{Q}^2)^3} \in [0,1] \quad (3)$$

where $\beta^2 = 0$ and $\beta^2 = 1$ mean, respectively, uniaxial and biaxial nematic textures.

In one spatial dimension, we define a physical domain $\Omega_p = [0,1]$ and a computational one $\Omega_c = [0,1]$; then we denote a PDEs solution over the physical domain $\Omega_p = [0,1]$ as $u(z,t)$, $z \in \Omega_p$, while if $\xi \in \Omega_c$ is a computational coordinate, we define a coordinate transformation from $\Omega_p \times (0,T]$ to $\Omega_c \times (0,T]$ as $\xi = \xi(z,t)$, and the reverse $z = z(\xi,t)$ holds. The integration domain is discretized with a fixed number of grid points, and the definition of the monitor function is based on a method proposed by Huang et al. [12], which ensures a good quality control of the meshes and final convergence of the FEM solution [13,14]

$$M(u(z,t)) = \int_0^1 \left(\left| \frac{\partial u(z,t)}{\partial z} \right| \right)^{1/2} dz + \left(\left| \frac{\partial u(z,t)}{\partial z} \right| \right)^{1/2} \quad (4)$$

The equidistribution of (4) [13,15] in each subinterval of the integration domain gives the mesh equation

$$M(z(x,t)) \frac{\partial}{\partial \xi} z(x,t) = \int_0^1 M(u(s,t)) ds = C(t) \quad (5)$$

and since at a larger monitor function value corresponds a denser mesh, a mesh map control with improved resolution is obtained.

Full details about the used multipass algorithm, numerical procedure and settings can be found in [3-6], we remark only that to solve (1) and (2) we replace the unknown $u(z,t)$ in (4), with $\text{tr}(\mathbf{Q}^2)$, a quantity which is rapidly varying when the degree of order is not constant; the physical domain has been discretized with a mesh of 285 grid points using the physical parameters typical for 5CB nematic liquid crystal at $\Delta T = -1^\circ\text{C}$ [16]. We modelled a one-dimensional asymmetric π -cell of thickness $1\mu\text{m}$, to which a rectangular electric pulse is applied perpendicularly to the plates at $t=0$ s for a duration $\Delta t = 0.25$ ms, sampling the dynamical evolution of the \mathbf{Q} tensor with a time step size $\delta t = 0.1$ μs .

3. Results and discussion

Recently we have shown [17], both experimentally and numerically, that applying an electric pulse to a 5CB NLC confined in an asymmetric π -cell, the arising distortion is relaxed through an increasing biaxial order close to the boundary plate where the anchoring angle is smaller, and to solve the PDEs system arising from the problem modelling we used the FEM based on a uniform discretization of the integration domain. In the present simulation, instead, we solve the PDEs system using the MMPDE technique to show as, enhancing the nematic frustration, a better resolution puts in evidence the relaxation mechanism observed close the boundary plates. In figure 2 we show the biaxiality maps obtained with $\theta_L = 19^\circ$ and $\theta_U = -3^\circ$, for amplitudes of the applied pulse of, respectively, 15 V/ μm (a), 22 V/ μm (b), 25 V/ μm (c) and 40 V/ μm (d), linearly mapped in a grey levels scale between the black (zero biaxiality) and the white (maximum biaxiality) colours. The vertical axis corresponds to the cell thickness, while in the horizontal one is represented the solution evolution in the $0 \text{ ms} \leq t \leq 0.1 \text{ ms}$ interval, in logarithmic scale for plotting convenience. In each panel of the figure, the inset shows the magnification, not spatially scaled, of the biaxiality within 15 nm under the upper boundary plate. At $t = 0 \text{ s}$, whatever the amplitude of the applied field is, close to the upper surface the nematic molecules

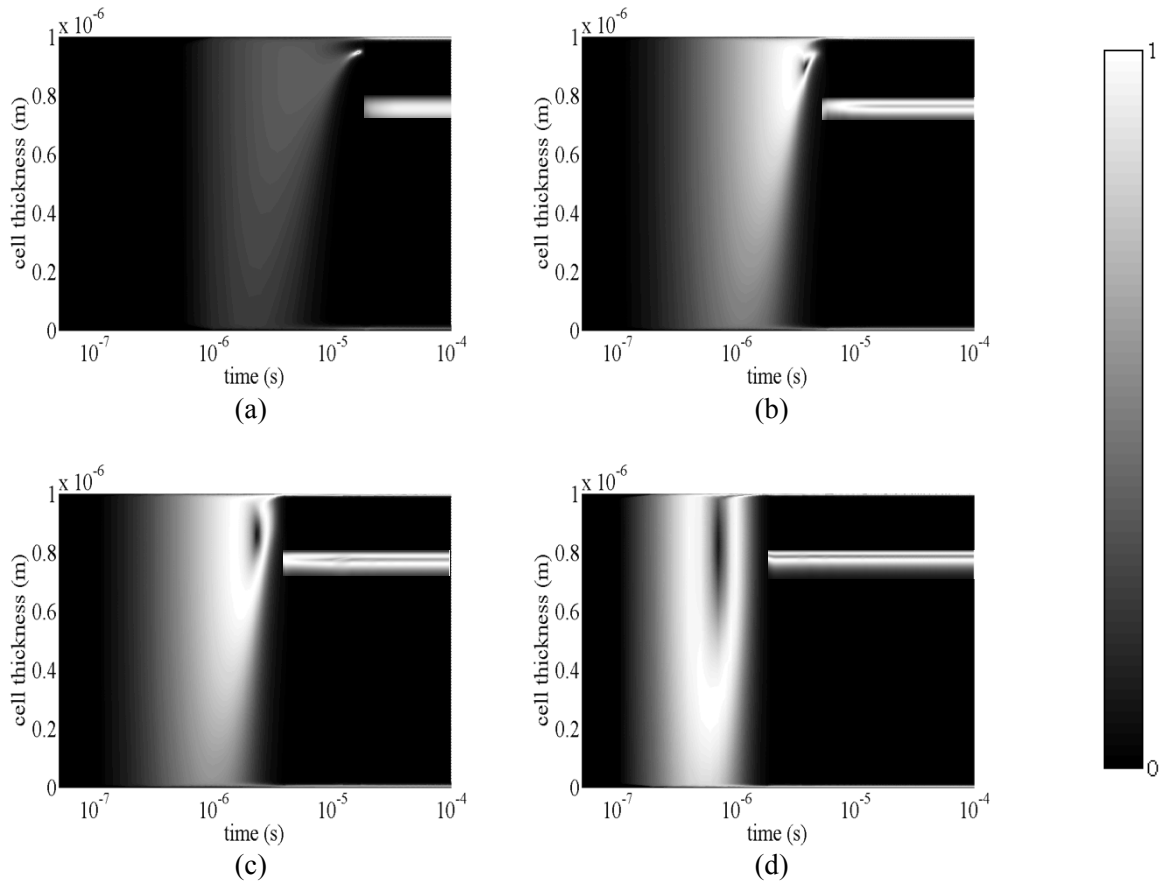


Figure 2. Surface contour plots of the biaxial order evolution for $\theta_L = 19^\circ$, $\theta_U = -3^\circ$, and electric pulse amplitudes of 15 V/ μm (a), 22 V/ μm (b), 25 V/ μm (c) and 40 V/ μm (d). The insets show the magnification of the biaxiality, not spatially scaled, within 15 nm under the upper boundary plate.

stay almost planar to the plate, while the bulk nematic texture has an asymmetric splayed configuration compatible with the prescribed boundary conditions. Applying a pulse of amplitude 15 V/ μm , figure 2(a), for $t > 0 \text{ s}$ the director starts to align along the field direction, while a biaxial region of thickness about 20 nm, hence comparable with ξ_b , connects the quasi-planar nematic texture lying

close to the upper surface, to the vertical nematic molecules located in the bulk: the nematic distortion tends towards the upper boundary plate where it relaxes by lowering the nematic order [3,17], and the starting uniaxial phase is locally replaced by growing biaxial domains. Just underneath the upper surface a bulk order reconstruction occurs around $t = 10 \mu\text{s}$, characterized by the ring-like biaxial region surrounding a planar uniaxial state [1]; for $t > 10 \mu\text{s}$ the initial splayed texture is replaced by a bend one, and a uniaxial order is restored everywhere except for the biaxiality growing close to the boundary surfaces, due to the anchoring conditions imposed: near the upper surface, in particular, the competition between the molecules lying in a quasi planar configuration and the nematic texture aligned vertically along the field direction induces a strong distortion which is relaxed by a growing biaxial wall [17], see the inset of figure 2(a). Increasing the pulse amplitude, it is well known that the biaxial structures become faster [5], and at the same time the bulk order reconstruction spreads progressively along the cell thickness, losing its cylindrical symmetry [6]: in the present case, as the competition between the quasi planar texture and the vertical one becomes stronger close to the upper boundary plate, inside the surface biaxial wall an order reconstruction transition occurs, lasting for the whole pulse duration, see the inset of figures 2(b)-2(d), concurring together the bulk order reconstruction transition to the relaxation of the textural distortion [18].

4. Conclusions

Our MMPDE simulations are consistent with previous computations and suggest that, although with different temporal durations, surface and bulk order reconstruction transitions cooperate to relax the textural distortions induced in frustrated NLCs confined in a π -cell with strong asymmetries as well as strong electric distortions. The afforded problem involves characteristic lengths and times with large-scale differences, and although it is simplified and in one space dimension, it is a useful model representative of higher-dimensional real problems, confirming the validity of our numerical method also in simulating markedly distorted physical systems as in the present case.

References

- [1] Barberi R, Ciuchi F, Durand G, Iovane M, Sikharulidze D, Sonnet A and Virga E G 2004 *Eur. Phys. J. E* **13** 61–71
- [2] Biscari P and Cesana P 2007 *Contin. Mech. Thermodyn.* **19** 285–98
- [3] Amoddeo A, Barberi R and Lombardo G 2012 *Phys. Rev. E* **85** 061705–10
- [4] Amoddeo A, Barberi R and Lombardo G 2010 *Comput. Math. Appl.* **60** 2239–52
- [5] Amoddeo A, Barberi R and Lombardo G 2011 *Liq. Cryst.* **38** 93–103
- [6] Amoddeo A, Barberi R and Lombardo G 2013 *Liq. Cryst.* **40** 799–809
- [7] de Gennes P G and Prost J 1993 *The Physics of Liquid Crystals* (Oxford: Clarendon Press)
- [8] Amoddeo A 2015 *Comput. Math. Appl.* **69** 610–9
- [9] Amoddeo A 2015 *Cogent Physics* **2** 1050080
- [10] Brimicombe P D and Raynes E P 2005 *Liq. Cryst.* **32** 1273–83
- [11] Virga E G 1994 *Variational Theories for Liquid Crystals* (London: Chapman and Hall)
- [12] Huang W, Ren Y and Russell R D 1994 *SIAM J. Numer. Anal.* **31** 709–30
- [13] Beckett G, Mackenzie J A, Ramage A and Sloan D M 2001 *J. Comput. Phys.* **167** 372–92
- [14] Beckett G and Mackenzie J A 2000 *Appl. Numer. Math.* **35** 87–109
- [15] de Boor C 1974 Good approximation by splines with variable knots II *Conf. on the Numerical Solution of Differential Equations (Dundee, UK, 1973) (Lecture Notes in Mathematics vol 363)* ed G A Watson (Berlin: Springer-Verlag) pp 12–20
- [16] Ratna B R and Shashidhar R 1977 *Mol. Cryst. Liq. Cryst.* **42** 113–25
- [17] Lombardo G, Amoddeo A, Hamdi R, Ayeb H and Barberi R 2012 *Eur. Phys. J. E* **35** 9711–16
- [18] Amoddeo A 2015 *Journal of Physics: Conference Series* **574** 012102